

行政院國家科學委員會專題研究計畫 成果報告

子計劃三：寬頻正交分頻調變傳輸系統之傳輸信號處理技術
研究及傳輸子系統整合(I)

計畫類別：整合型計畫

計畫編號：NSC91-2219-E-009-010-

執行期間：91年08月01日至92年07月31日

執行單位：國立交通大學電子工程研究所

計畫主持人：陳紹基

報告類型：完整報告

處理方式：本計畫涉及專利或其他智慧財產權，2年後可公開查詢

中 華 民 國 92 年 11 月 9 日

行政院國家科學委員會補助專題研究計畫 成果報告
 期中進度報告

(計畫名稱)

基於正交分頻多重進接之無線多媒體傳收機研究及設計-子計劃三:寬頻正交
分頻調變傳輸系統之傳輸信號處理技術研究及傳輸子系統整合(I)

計畫類別： 個別型計畫 整合型計畫

計畫編號：NSC91-2219-E-009-010-

執行期間：91年8月1日至92年7月31日

計畫主持人：陳紹基

共同主持人：

計畫參與人員：卓建宏、葉顏輝、鄭光甫、黃崇倫、鄭元容、曲建全

成果報告類型(依經費核定清單規定繳交)： 精簡報告 完整報告

本成果報告包括以下應繳交之附件：

- 赴國外出差或研習心得報告一份
- 赴大陸地區出差或研習心得報告一份
- 出席國際學術會議心得報告及發表之論文各一份
- 國際合作研究計畫國外研究報告書一份

處理方式：除產學合作研究計畫、提升產業技術及人才培育研究計畫、
列管計畫及下列情形者外，得立即公開查詢

涉及專利或其他智慧財產權， 一年 二年後可公開查詢

執行單位：交通大學電子研究所

中華民國 92 年 10 月 25 日

中文摘要:

本年共完成諸多研究成果如下：(1) 我們首先對現有諸多通道估測及等化演算完成其應用於 802.16a 之效能模擬及評估；(2) 我們提出兩個以 DCT 轉換為基本演算之通道內插及估測法，其比傳統以 DFT 為主之方法效能更佳；(3) 我們提出兩個在快速衰減環境下之 ICI 消滅法及通道估測法，其比現有方法有更佳效能；(4) 我們提出一 OFDM 軟體無線電基頻架構其可以低硬體成本達成多模式、多標準之可重組及可程式化接收。

關鍵詞：正交分頻調變、同步、中頻、快速傅立葉轉換、軟體無線電、IEEE 802.16 標準、IEEE 802.11a 標準、數位信號處理器、數位信號降頻、多速率數位調變

英文摘要:

This projects accomplished the following results: (1) performance verification and evaluations of the existing channel estimation methods are completed; (2) two high-performance DCT-based channel interpolation methods are proposed, which have better results than the popular DFT-based methods; (3) two fast-fading channel estimation methods are proposed which have better performance than the existing methods; and (4) an OFDM-based SDR receiver architecture is proposed, which can be reconfigured for the operations of varying modes and standards with low complexity and overhead.

Keywords : OFDM, Synchronization, IF, FFT, Software-Defined Radio, IEEE 802.16 standard, IEEE 802.11a standard, Digital Signal Processor, Digital Down Conversion, Multi-rate Digital Demodulation

I. Preface

OFDM is an efficient transmission scheme, which has the merits of high transmission rate, high robustness to inter-symbol interference and easy equalization of channel effect. There it is adopted in various current and future state-of-art wired or wireless communication systems, such as ADSL, VDSL, 802.16, 802.11a, DVB, and DAB. However, OFDM scheme suffers from fast-fading effect, inter-carrier-interference effect. It also required high-accuracy channel estimation and timing synchronizations (including accurate frequency offset estimation, symbol timing synchronization and sampling clock synchronization). Those problems are the key OFDM design issues for its practical low-cost realization. Meanwhile, the mentioned OFDM systems cover various applications ranging from wired internet access (due to ADSL and VDSL), WMAN, WLAN, and consumer wireless audio and video accesses. Therefore it is beneficial to integrate and combine those systems within a single baseband platform for seamless integration those systems for an obstacle-free and transparent wideband cyber roaming.

II. Objectives

This project is the third subproject of the project “OFDMA-Based Mobile Wireless Multimedia Transceiver Research and Design). It is aimed to investigate high-performance unified digital signal processing techniques for broadband OFDM-based transceivers. Unification means efficient programmable and configurable design of DSP techniques for multi-mode and/or multi-standard transceiving, subject to maximizing the utilization of a common sharable OFDM core architecture. The project is also responsible for the integration of the whole transmission subsystem, which includes this subproject and subproject 4. Problems to be investigated include: high-performance transceiver filtering, high-performance synchronization technique, high-performance multi-carrier modulation and demodulation techniques for broadband applications, and the design of advanced digital IF-band signal processing down-converted to baseband signal, with the consideration of software-radio concept for multi-mode and/or multi-standard and multi-bandwidth applications. Some broadband OFDM-based wireless communication systems, specifically the WirelessMAN standards 802.16a and 802.16b for wireless “last-mile” internet access, and the WLAN 802.11a will be considered for the unified design.

III. Investigation of Current Designs

(a) The Wiener’s channel interpolation

The frequency-domain Wiener channel interpolator [1] can be derived from the following LMMSE estimation algorithm as shown below:

$$\text{Min} \left\{ E \left[\left(\underline{H}(m) - \sum_p C(m, p) \hat{H}(p) \right)^2 \right] \right\} = E \left[\left(\underline{H}(m) - \sum_p C(m, p) \hat{H}(p) \right) \underline{H}(p')^* \right]$$

where m is data carrier index, p and p' indicate pilot carrier indices

$$E \left[\sum_p C(m, p) \hat{H}(p) \hat{H}(p')^* \right] = E \left[H(m) \hat{H}(p')^* \right]$$

$$\sum_p C(m, p) \underbrace{\left[R_f(p - p') + \frac{NO}{Es} \delta(p - p') \right]}_{R_{\hat{H}p\hat{H}p'}} = \underbrace{R_f(m - p')}_{R_{Hm\hat{H}p'}}$$

$\hat{H}p$: pilot vector ; $\hat{H}p$: pilot value

Finally, we obtain the Wiener interpolator $C(m)$ as $C(m) = R_{\hat{H}p\hat{H}p}^{-1} R_{Hm\hat{H}p}$

(b) Linear channel interpolation

$$\hat{H}(mM + \ell) = \frac{M - \ell}{M} \hat{H}_{LS}(mM) + \frac{\ell}{M} \hat{H}_{LS}((m+1)M), \quad 0 < \ell < M$$

(c) The second-order polynomial channel interpolation

$$\begin{aligned} \hat{H}(mM + \ell) &= \frac{(\ell - M)(\ell - 2M)}{(0 - M)(0 - 2M)} \hat{H}_{LS}(mM) + \frac{(\ell - 0)(\ell - 2M)}{(M - 0)(M - 2M)} \hat{H}_{LS}((m+1)M) \\ &+ \frac{(\ell - 0)(\ell - M)}{(2M - 0)(2M - M)} \hat{H}_{LS}((m+2)M), \quad 0 < \ell < 2M \end{aligned}$$

It fits two data areas between three pilots with a parabola curve, thus offers a better performance than linear interpolation. Besides, from simulation we find that, the higher order polynomial interpolation is used, the more fluctuation it will be. In [2], the author pointed out the most appropriate polynomial interpolation is spline of order 3 (i.e., is cubic spline).

(d) Spline channel interpolation [2]

Quadratic Spline interpolation was developed under the consideration that signals commonly have some degree of continuity in physical world. The interpolation scheme is based on second-order polynomial that ensures continuity of an interpolation point. The interpolation process starts with $N^s + 1$ -point scattered pilot carriers obtained by LS estimation.

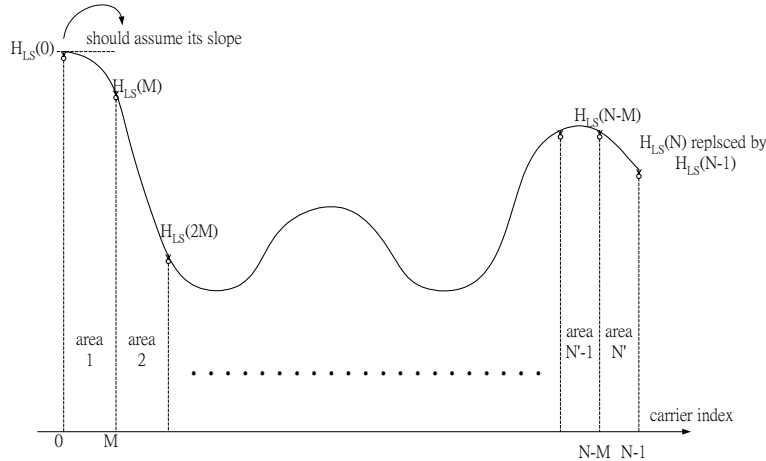


Figure 1. Illustration of channel segment

Then all the other carriers in the N^s divisions created by these scattered pilots can be interpolated by using the LS estimates. More precisely, the channel estimates in the i -th division can be obtained by the second-order interpolation function $Y_i = Ax_i^2 + Bx_i + C$. To solve the total $3N^s$ unknowns, we need $3N^s$ equations. They can be set up by considering the two known boundary pilot values in each division, and continuity of the first derivative value of boundary channel estimate separating two divisions. Consequently, totally we have $(2N^s) + (N^s - 1)$ known equations. The re-

maintaining one equation can be obtained by assuming that the first carrier point in the 1st division has zero slope (nature type) or slope= $[pilot(1) - pilot(0)]/M$.

For generalization, we can have high-order spline functions such as the widely used ‘‘Cubic Spline’’ for channel interpolation. It is based on the 3rd-order curve-fitting polynomial $Y_i = Ax_i^3 + Bx_i^2 + Cx_i + D$. Hence there are total $4N'$ unknowns. All the divisional polynomial coefficients are solved similarly to the quadratic case, plus considering the 2nd derivative continuity of the division separation pilot channel values. Therefore, we can set up $(2N') + (N' - 1) + (N' - 1)$ equations from the constraints, plus two more from the assumption of zero 1st derivative value of the very first and last carrier channel value.

(e) Other channel interpolations

The DFT-based channel interpolations [3], [4] are popular and effective. They are based on the ideal LTI interpolation theory in frequency domain. However, the methods are poor when applied to non-sampled-spaced channels. On the other hand, the interpolation using the sinc function is based on the idea of optimal time domain low-pass filtering. The approach is impractical due to Gibbs phenomenon and slow-decay of sinc coefficients.

IV. The Proposed Methods and Results

(a) Performance evaluation of some key existing channel interpolation schemes

We simulate the previously mentioned channel interpolation techniques assuming channel impulse with exponentially decayed power. The channel taps of our simulation are assumed sample-spaced and pilot allocations are equally spaced. The results are shown in Figure 1.

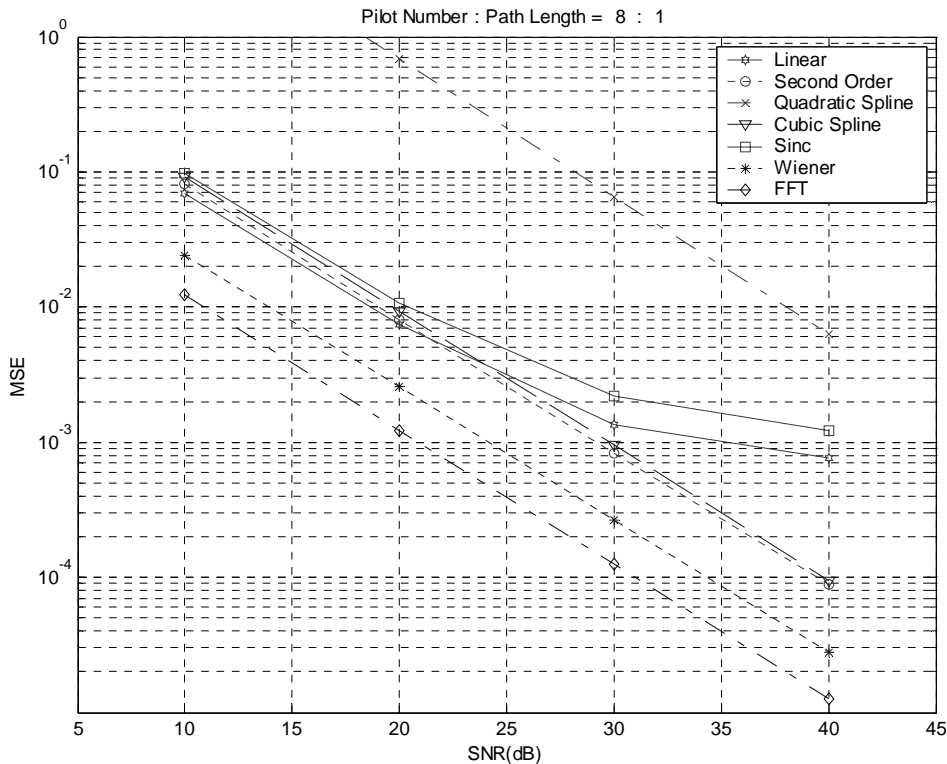


Figure 1. MSE comparison of several channel interpolation techniques

We first notice the quadratic spline interpolation function unexpectedly performs the worst among all. It can be reasonably explained as that when noise added to the pilot-carriers, the noise affects not only the pilot-carrier's neighborhood but also whole region, due to the reason that we assume the continuity of channel. Similarly, cubic spline technique performs just a little better than the lower-complexity second order interpolation. As for case of longer path lengths, the MSE performance of Wiener interpolation technique performs worse than cubic spline. This can be seen as the effect of model mismatch of channel statistics. In addition to MSE performance, we compare their complexity in Table 1.

Table 1. Comparison of computation complexities of several channel interpolation techniques

Computation Complexity for each carrier	
Linear Interpolation	4 MPYs + 2 Adds
Second-Order Interpolation	4MPY + 4 Adds
Quadratic Spline	4MPY + 4 Adds
Cubic Interpolation	At least 6MPY + 6Adds
Sinc Interpolation	$2 * O((Kc/M)^2)MPY +$ $2(Kc/M-1)Adds$
Wiener Interpolation	$2 * O(P^2)MPY +$ $2(P-1)Adds$
FFT Interpolation	$\log_2 N + 1/N * (\log_2 P)$

Considering the MSE performance in Figure 1 and computation complexity in Table 1, we conclude that the second-order interpolation is effective than in terms of performance and cost.

(b) Two new DCT-based channel interpolation methods

When performing DFT on a set of N -point data, it is equivalent to periodically extend the N -point data to infinite length and then transform it by discrete time Fourier transform (DTFT). Therefore, if it is discontinuous between two ends of the N -point data, there will be abrupt variation in between consecutive periods after extension and high frequency component will rise in the transform domain. By the interpolation concept, high frequency component is usually the source of aliasing and must be prevented as much as possible. Therefore, in this case, we have a high tendency of getting error-prone interpolated channel frequency samples, and this is why the estimation will be poor by using DFT-based interpolator if the channel has non-sample-spaced path delay times.

Compared with DFT, DCT can reduce high frequency component in the transform domain by eliminating the edge effect as mentioned above. The reason is that operation of N -point DCT is equivalent to extend the original data to $2N$ -point by mirror-duplication and then perform $2N$ -point DFT on the extended data followed by constant magnitude and phase compensation. Obviously, mirror -duplication can solve the discontinuity problem introduced by periodic extension. Therefore, DCT indeed has better power concentration at low frequency. This benefits interpolation process. In the following We propose two DCT-based estimators. The first one is DCT/EIDCT-based channel estimator [5] as shown in Figure 2.

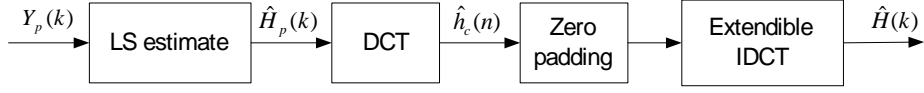


Figure 2. The 1st new DCT/EIDCT-based channel estimator

The operation of extendible IDCT is

$$\hat{H}(k) = \sum_{m=0}^{M-1} w(m) \hat{h}_c(m) \cdot \cos\left(\left(\frac{k}{N} + \frac{1}{2M}\right)\pi m\right) \quad k = 0, 1, 2, \dots, N-1$$

where M is the original data length and N is the data length after interpolation.

The second DCT-based estimator is IDCT/DCT-based channel estimator. The block diagram of this estimator is shown in Figure 3.

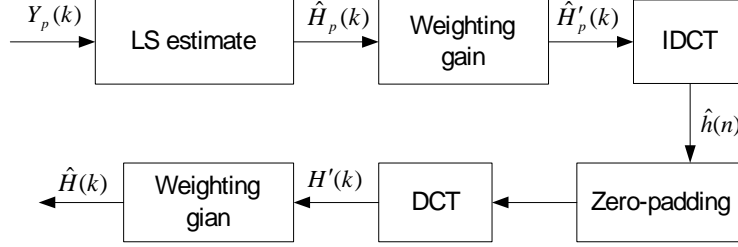


Figure 3. The 2nd new IDCT/DCT-based channel estimator

where the 1st and 2nd weighting gain operations are respectively:

$$\hat{H}'_p(k) = \begin{cases} \frac{1}{\sqrt{2}} \hat{H}_p(k) & k = 0 \\ e^{-\frac{j\pi k}{2M}} \hat{H}_p(k) & 1 \leq k \leq M-1 \end{cases}, \quad \hat{H}(k) = \begin{cases} \frac{1}{\sqrt{2}} H'(k) & k = 0 \\ e^{\frac{j\pi k}{2N}} H'(k) & 1 \leq k \leq N-1 \end{cases}$$

Among these two estimators, the DCT/EIDCT-based has better performance. Although IDCT/DCT-based estimator has a little performance degradation, it has the advantage of direct implementation by conventional DCT and IDCT hardware and software.

To evaluate performance of the proposed new channel estimator, here we use a channel with non-sample-spaced multipath delay times to simulate the performance of the two estimators. Figure 4 shows the SER of the DCT/EIDCT-based channel estimator, along with the DFT-based estimator and robust LMMSE estimator. We can find that DCT/EIDCT-based has better performance than DFT-based estimator at high SNR and has the performance close to robust LMMSE estimator. The error floor of DFT-based estimator is due to the aliasing effect. The DCT/EIDCT-based estimator can exactly solve the problem and reduce the error floor. Figure 5 shows the SER performances of IDCT/DCT-based estimator. The performance of IDCT/DCT-based estimator is a little worse than DCT/EIDCT-based estimator but still better than DFT-based estimator. Therefore, for the implementation issue, it's a good choice.

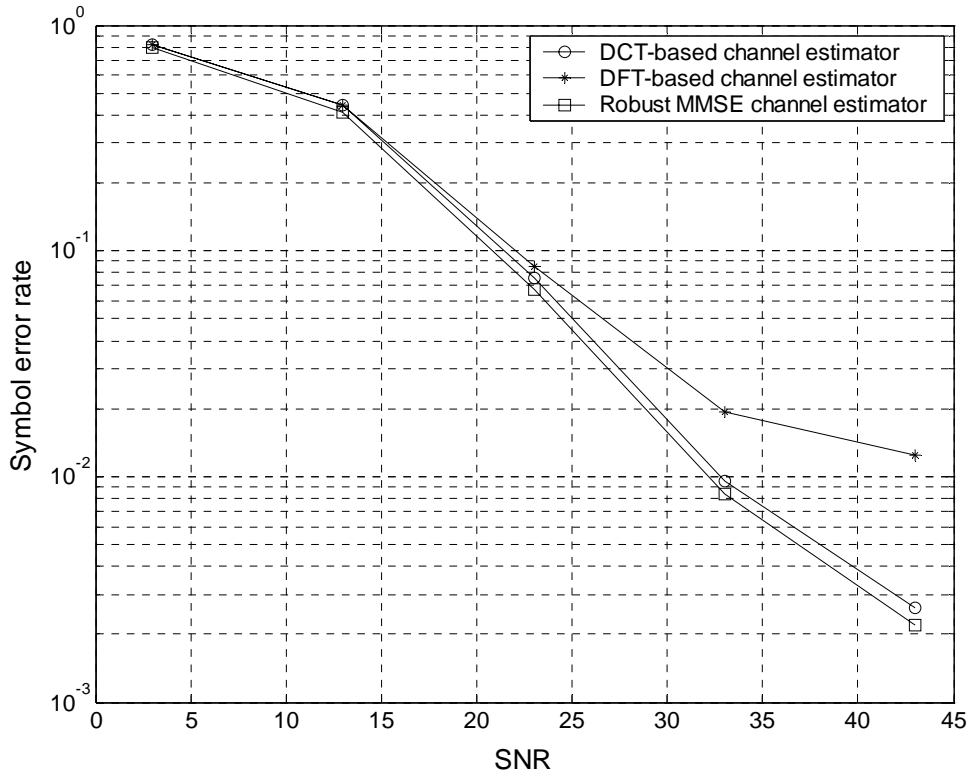


Figure 4. SER performances of DFT-based and DCT-based channel estimators.

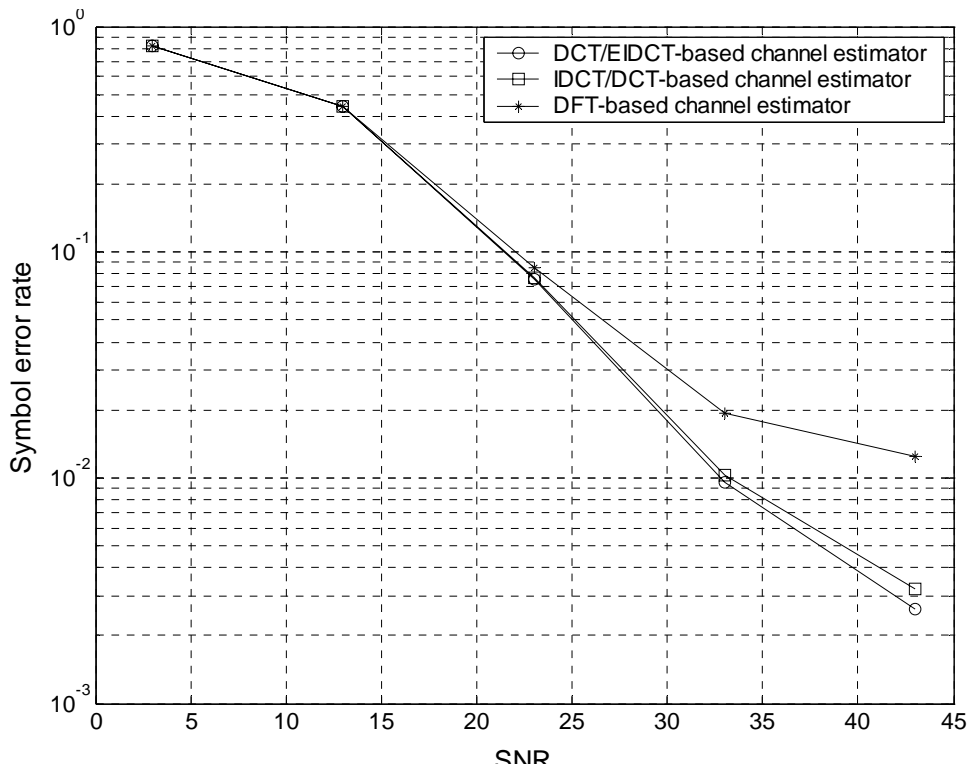


Figure 5. SER performance of IDCT/DCT-based channel estimator

(c) Two new channel estimation methods for fast-fading channels

The first fast-fading channel estimation algorithm flow is shown in Fig. 6 and described as follows.

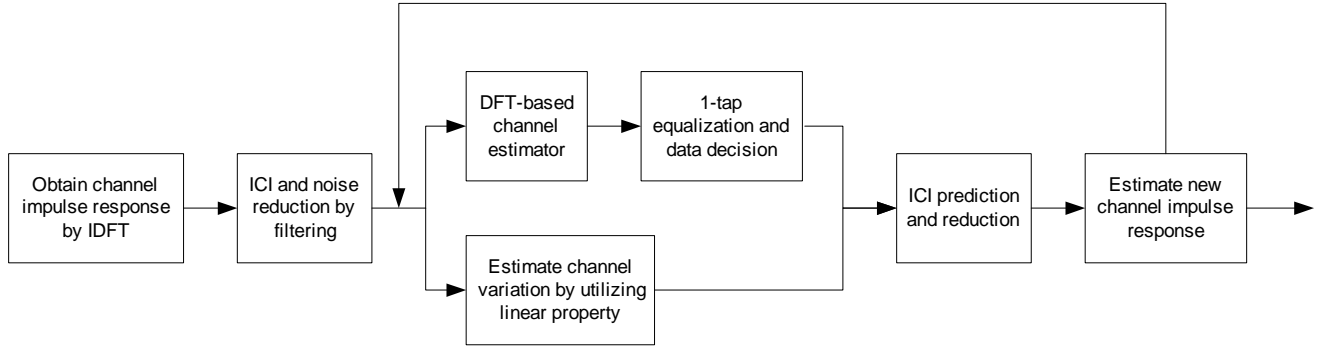


Figure 6. Block diagram of the proposed fast-channel estimation method

The algorithm steps:

1. Assumed i is the symbol index, $Y_{i,p}(m)$ is the pilot subcarrier, M is the number of pilot subcarriers.

$$Y_i^{(0)}(m) = Y_i(m) \quad Y_{i,p}^{(0)}(m) = Y_{i,p}(m) = Y_i\left(\frac{N}{M}m\right), \quad I = 0$$

2. Estimate channel impulse response $\hat{\mathbf{h}}_i$ for the i -th symbol by performing IDFT on frequency responses at pilot subcarriers, which are obtained by 1-tap division

$$\hat{\mathbf{h}}_i = IDFT\{\hat{H}_{i,p}^{(0)}(m)\}, \quad \hat{H}_{i,p}^{(0)}(m) = \frac{Y_{i,p}^{(0)}(m)}{P(m)}, \quad m = 0, 1, 2, \dots, M-1$$

3. To reduce ICI and noise effect on the channel impulse estimate, a smoothing filter or LMMSE can be applied to consecutive symbols [6]. After ICI and noise reduction, estimate of channel impulse response for the i -th symbol is defined as $\hat{\mathbf{h}}_i^{(0)}$.

4. Perform DFT-based channel estimation using $\hat{\mathbf{h}}_i^{(0)}$. Then use the estimated channel frequency response, $\hat{H}_i(m)$, to equalize $Y_i^{(l)}(m)$, i.e., $\hat{Y}_i^{(l)}(m) = \frac{Y_i^{(l)}(m)}{\hat{H}_i(m)}$, $m = 0, 1, 2, \dots, N-1$.

After that, decisions are made to yield $\hat{d}_i(m)$

5. For the i -th symbol, the difference between $\hat{\mathbf{h}}_i^{(l)}$ and $\hat{\mathbf{h}}_{i-1}^{(l_{\max})}$ is used to derive s_i .

$\hat{\mathbf{h}}_{diff,i} = \hat{\mathbf{h}}_i^{(l)} - \hat{\mathbf{h}}_{i-1}^{(l_{\max})}$. $\hat{\mathbf{h}}_{i-1}^{(l_{\max})}$ is the estimated channel impulse response for the $(i-1)$ -th symbol, which has been processed by this ICI-reduction algorithm. Then with the assumption that channel variation during two consecutive OFDM symbols is linear, we can estimate s_i

for the i -th symbol by $\hat{\mathbf{s}}_i = \hat{\mathbf{h}}_{diff,i} \times \frac{T}{T_s} \times \frac{1}{N}$, $\hat{\mathbf{s}}_i = [\hat{s}_{i,0} \quad \hat{s}_{i,1} \quad \hat{s}_{i,2} \quad \dots \quad \hat{s}_{i,M-1}]^T$

where T_s is the complete OFDM symbol duration including cyclic prefix. Then estimate \hat{s}_l of s_l can be calculated by dividing $\hat{\mathbf{h}}_{diff,i}$ by the number of total samples within a complete OFDM symbol.

6. With the information of \hat{s}_i and $\hat{d}_i(m)$, ICI can be predicted and reduced by performing

$$Y_i^{(I+1)}(m) = Y_i^{(0)}(m) - \frac{1}{N} \sum_{k \neq m} \left[\hat{d}_i(k) L(m-k) \left(\sum_{l=0}^{M-1} \hat{s}_{i,l} e^{-j \frac{2\pi k l}{N}} \right) \right], \quad m = 0, 1, 2, \dots, N-1$$

Then use this ICI-reduced signal to yield new channel impulse response

$$\hat{\mathbf{h}}_i^{(I+1)} = IDFT\{\hat{H}_{i,p}^{(I+1)}(m)\}, \hat{H}_{i,p}^{(I+1)}(m) = \frac{Y_{i,p}^{(I+1)}(m)}{P(m)}, \quad m = 0, 1, 2, \dots, M-1$$

This completes the I -th iteration.

7. End if $I = I_{\max}$, otherwise $I = I + 1$ and repeat Steps 4-7.

In the performance simulation, we assume 16QAM data. The number of total subcarriers $N = 64$, the total bandwidth 500KHz, the sampling period $T_c = 2\mu s$, and the length of cyclic prefix $T_g = 4T_c$. The multipath channel is assumed sample-spaced with $\nu = 4$ with exponentially-decayed power profile. There are 4 equispaced pilot subcarriers. Figure 7 shows the SER performance for the case $f_d T = 0.04$ with $I_{\max} = 3$. As shown, the ICI-reduction algorithm effectively reduces the error floor.

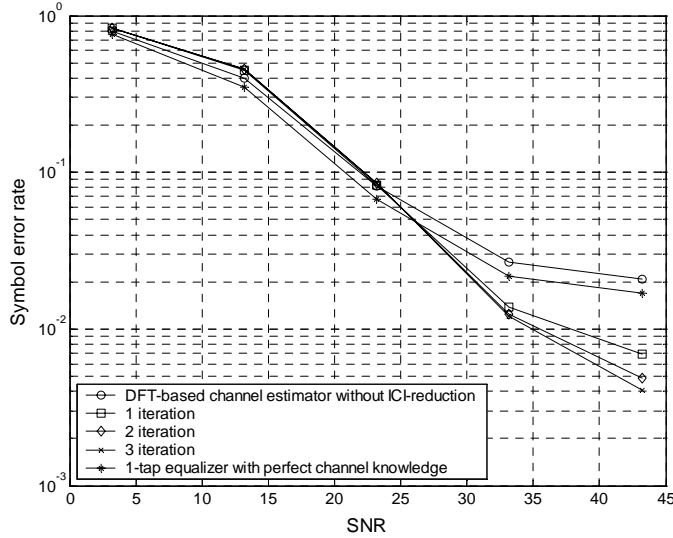


Figure 7. SER performance of Doppler-induced ICI reduction algorithm, $f_d T = 0.04$

The second new fast-fading channel estimation method is based on the reasonable assumption that for $f_d T$ is less than 0.1, the channel variation over an OFDM symbol can be assumed linear

[7], [8], where f_d is the Doppler frequency and T is the OFDM symbol duration. With this assumption, the time-variant channel impulse response can be written as $h(n,m) = \sum_{l=0}^{\nu-1} (s_l n + a_l) \delta(m-l)$

and DFT of the received signal can be written as

$$Y(m) = \frac{1}{N} \sum_{l=0}^{\nu-1} s_l \sum_{k=0}^{N-1} d(k) L(m-k) e^{-j\frac{2\pi k m}{N}} + d(m) \sum_{l=0}^{\nu-1} a_l e^{-j\frac{2\pi k m}{N}} + \tilde{N}(m) \quad m=0,1,\dots,N-1$$

where s_l and a_l are the variation slope and initial value of the path gain, and $L(k)$ is

$$L(k) = DFT\{n\} = \begin{cases} N(N-1)/2 & m = 0, \pm N, \pm 2N, \dots \\ \frac{jN}{2 \sin(\frac{\pi k}{N})} e^{j\pi k / N} & otherwise \end{cases}$$

To solve the channel parameter, by considering the strong correlation between the ICI's, we first perform the following operations to reduce ICI significantly reduced.

$$Y(m) - Y(m+1) = \frac{1}{N} \sum_{l=0}^{\nu-1} s_l \sum_{k=0}^{N-1} d(k) [L(m-k) - L(m+1-k)] e^{-j\frac{2\pi k m}{N}} + \sum_{l=0}^{\nu-1} a_l \left[d(m) e^{-j\frac{2\pi k m}{N}} - d(m+1) e^{-j\frac{2\pi k (m+1)}{N}} \right] + \tilde{N}(m) - \tilde{N}(m+1)$$

From this set of differential equations, we form a linear system for parameters s_l and a_l . From which we can achieve accurate modeling of fast channel, and accordingly achieve effective channel estimation and demodulation process. Fig. 8 shows the simulation results of the proposed method, in comparison with the method of [9]. As shown the new method has better performance.

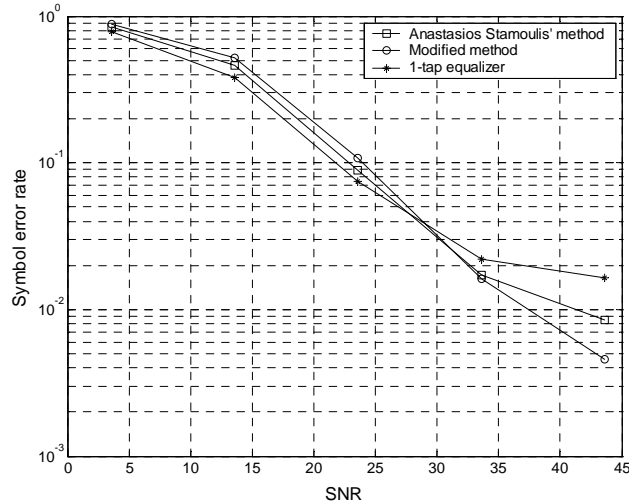


Figure 8. SER comparison of the method in [9] (4ν pilots) and the new method (3ν pilots), $f_d T = 0.04$

(d) A unified multi-mode and multi-standard SDR baseband inner receiver

Basically the proposed receiver architecture is cost and performance effective, and can be flexibly reconfigured for multi-mode and multi-standard OFDM operations, with low overhead and small area. Due to page limitation, we will not detail the architecture of our design.

IV. Conclusion

In this project, we generally completed all the tasks originally planned. We have proposed many efficient baseband signal processing techniques for OFDM systems, particularly for channel estimation. In addition, we also produced some extra new results not committed in the original

proposal. Due to page limitation, some more new findings are not covered here, such as those related OFDM synchronization. As of this writing, we have published one conference paper in ICASSP03 and submitted two papers to ICC04 and one paper to ICASSP04. Meanwhile, we are in the process of writing up the detailed results and submitting them to journals.

References

- [1] P. Hoeher, S. Kaiser and P. Robertson, "Two-dimensional pilot-symbol-aided channel estimation by Wiener filtering," ICASSP, Vol: 3, Page(s): 1845 -1848 April 1997
- [2] R. D. Harding and D. A. Quinney, A simple introduction to numerical analysis: interpolation and approximation, Adam Hilger 1989
- [3] Y. Zhao and A. Huang, "A Novel Channel Estimation Method for OFDM Mobile Communication Systems Based on Pilot Signals and Transform-Domain Processing," *Proc. VTC'97*, pp. 2089-2094.
- [4] B. Yang, K. B. Letaief, R. S. Cheng, and Z. Cao, "Windowed DFT Based Pilot-symbol-Aided Channel Estimation for OFDM Systems in Multipath Fading Channels," *Proc. VTC'00-Spring*, vol. 2, pp.1480-1484.
- [5] Y. F. Hsu and Y. C. Chen, "Rational interpolation by extendible inverse discrete cosine transform," *Electronics Letters*, vol. 33, no. 21, pp. 1774-1775, 9 Oct. 1997.
- [6] A. A. Hutter, R. Hasholzner, and J. S. Hammerschmidt, "Channel Estimation for Mobile OFDM Systems," *IEEE VTC'99-Fall*, vol. 1, pp. 305-309.
- [7] W. G. Jeon, K. H. Chang, and Y. S. Cho, "An Equalization Technique for Orthogonal Frequency-Division Multiplexing Systems in Time-Variant Multipath Channels," *IEEE Trans. Comm.*, vol. 47, no. 1, Jan. 1999.
- [8] J. Li and M. Kavehrad, "Effect of Time Selective Multipath Fading on OFDM Systems for Broadband Mobile Application," *IEEE Comm. Letters*, vol. 3, no. 12, pp. 332-334, Dec. 1999.
- [9] A. Stamoulis, S. N. Diggavi, and N. A. Dahir, "Estimation of fast fading channels in OFDM," *IEEE WCNC*, vol.1, pp. 465-470, March 2002.